ACS Sustainable Chemistry & Engineering

pubs.acs.org/journal/ascecg

Research Article

Lactic Acid-Derived Copolymeric Surfactants with Monomer Distribution Profile-Dependent Solution and Thermoresponsive Properties

Nicola Migliore, Aleksander Guzik, Marc C. A. Stuart, Marc Palà, Adrian Moreno, Gerard Lligadas, and Patrizio Raffa*

Cite This: *ACS Sustainable Chem. Eng.* 2022, 10, 14806−14816

Read Online

ACCESS | Metrics & More | Article Recommendations | Supporting Information

ABSTRACT: We report the synthesis and solution properties of novel biobased thermoresponsive amphiphilic copolymers prepared using *N*,*N*-dimethyl lactamide acrylate (DMLA) and ethyl lactate acrylate (ELA) as hydrophilic and hydrophobic monomers, respectively. Copolymers with similar overall molecular weight but different monomer distribution profiles, such as random, diblock, triblock, and random−blocks, were prepared using photoinduced electron/energy transfer-reversible addition−fragmentation chain transfer (PET-RAFT) polymerization activated by a Zn-based photoredox catalyst. The synthesized polymers show interesting self-assembly and thermoresponsive behavior in water, depending on the monomers distribution along the chain. Different critical solution temperatures, in the range of 13−70 °C, were observed by tuning the monomers molar ratio and distribution. The formation of aggregates of various types was proven by transmission electron microscopy (TEM). The prepared polymers also display different surface activity with the fully random copolymer being significantly more surface active than block systems. A study of emulsion stabilization was performed with oils of various polarity, showing promising results for applications of these novel polymers as biobased surfactants and water/oil (w/o) emulsion stabilizers.

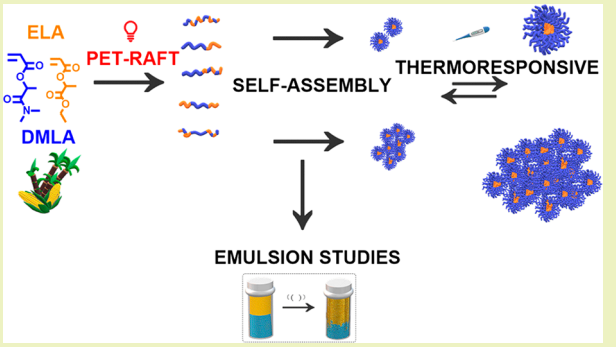

KEYWORDS: *PET-RAFT, Amphiphilic polymers, Polymeric surfactants, Thermoresponsive, Bioderived, Self-assembly, Green solvent*

INTRODUCTION

The synthesis of new materials from biobased sources is a relevant topic in polymer research, especially since concerns about climate change and sustainability have arisen.[1−4] The starting materials can be either biopolymers, such as starch[5−7] and lignin,[4,8,9] or bioderived monomers[10−16] that can be further polymerized. Particularly interesting results have been achieved with biobased (meth)acrylic derivatives.[17−20] This is because the broad range of pendant groups available allows fine-tuning of properties of the corresponding polymers, enabling their use in various different materials such as bioplastics, superabsorbent polymers, coatings, and paint formulations.[21−25] Biobased poly(meth)acrylates can be synthesized from many natural synthons such as glucose, fatty acids, glycerol, terpenes, and others.[21] Recently, neoteric lactic acid derivatives have also been considered in this respect.[18−20]

Lactic acid is obtained as a product from carbohydrates fermentation[26,27] or chemo-catalytic processes.[28−30] As a building block, it is mainly known as a monomer for the synthesis of biodegradable polymer poly(lactic acid) (PLA), one of the most successful bioplastics that is used in different fields such as food packaging,[31,32] cosmetics,[33] biomedical materials,[34] and others.[35,36] Lactic acid can also be converted into fine and commodity chemicals, making it one of the most known biobased platform chemicals.[21,37] In this respect, ethyl lactate (EL) and *N*,*N*-dimethyl lactamide (DML) are well-recognized green biosolvents that can be easily converted into their respective (meth)acrylate derivatives; these can subsequently be polymerized to yield homopolymers and block copolymers with different intrinsic properties.[20,38−40] In particular, as EL is hydrophobic and DML is hydrophilic, their copolymers can be amphiphilic.

Amphiphilic polymers have received great attention in the last three decades due to their ability to self-assemble into stable micelles or other aggregates in a selective solvent.[41−45] This makes them suitable for use in special applications such as drug delivery or enhanced oil recovery.[46−48] A typical technological

Received: July 21, 2022
Revised: October 12, 2022
Published: October 28, 2022

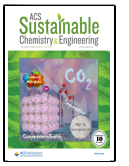

application of amphiphilic polymers is emulsion stabilization, as they prevent formulation breakdown mechanisms such as flocculation and coalescence.[49,50] Such polymeric surfactants offer many performance advantages over conventional ones and are increasingly employed to guarantee formulation stability in the challenging applications mentioned above. Polymeric surfactants impart excellent particle stability via steric stabilization, as the repulsive barriers of the polymer chains are better able to prevent coalescence and agglomeration. In both aqueous and nonaqueous dispersions, the multiple anchoring points of polymeric surfactants provide a superior interaction between surfactant and substrate. Combined with steric stabilization, this results in highly robust and stable formulations. Polymeric surfactants are therefore able to stabilize even highly loaded suspensions and still maintain viscosity at acceptable levels.[46,51−60]

In this work, we report the value enhancement of lactic acid-based solvents by transforming EL and DML to a series of green copolymeric surfactants based on random and block copolymers containing homopolymer or homopolymer/mixed segments. The combination of ethyl lactate acrylate (ELA) and *N*,*N*-dimethyl lactamide acrylate (DMLA) monomers and photoinduced electron/energy transfer-reversible addition−fragmentation chain transfer (PET-RAFT) polymerization enabled the precisely production of a series of innovative amphiphilic copolymeric surfactants with identical acrylic backbone structure but different distribution profiles of groups having different water affinities (i.e., ethyl ester and dimethyl amide).[57−59] Despite their overall compositions and molar masses being similar, copolymers with different composition profiles ranging from a poly(DMLA-r-ELA) random copolymer (**R**) to a poly[(DMLA-r-ELA)-*b*-DMLA-*b*-(DMLA-r-ELA)] triblock copolymer (**RBR**) with outer random segments showed remarkable differences in surface activity and aggregation behavior. Unexpectedly, some of them also showed thermoresponsive aggregation behavior, thus broadening their potential applications as stimuli responsive polymers.[52,60−62] Additionally, considering the surfactant properties, surface tension measurements and an emulsions stability study with different oils were performed to evaluate the potential of these biobased materials in related industrial applications.

EXPERIMENTAL SECTION

Materials. Carbon disulfide (Sigma-Aldrich, anhydrous, ≥99%), potassium bromate (Sigma-Aldrich, ACS reagent, ≥99.8%), potassium bromide (Sigma-Aldrich, ReagentPlus, ≥99.0%), potassium iodide (Sigma-Aldrich, ReagentPlus, 99%), sodium thiosulfate (Sigma-Aldrich, ReagentPlus, 99%), 1-butanethiol (Sigma-Aldrich, 99%), methyl 2-bromopropionate (Sigma-Aldrich, 98%), 1,4-phenylenebis(methylene) didodecyl dicarbonotrithioate (BM1812, Boron Molecular, 95%), 5,10,15,20-tetraphenyl-21*H*,23*H*-porphine zinc (ZnTPP, Sigma-Aldrich, 98%), 2,2′-azobis(2-methylpropionitrile) (AIBN, Sigma-Aldrich, 98%), *N*,*N*-dimethylformamide (DMF, Sigma-Aldrich, for HPLC, ≥99.9%), anisole (Sigma-Aldrich, anhydrous, 99.7%), dimethyl sulfoxide (DMSO, Sigma-Aldrich, dried ≤0.02% water), chloroform (Sigma-Aldrich, contains 100−200 ppm amylenes as stabilizer, ≥99.5%), acetone (Sigma-Aldrich, ACS reagent, ≥99.5%), petroleum ether (Sigma-Aldrich, anhydrous), toluene (Sigma-Aldrich, ACS reagent, ≥99.5%), ethanol (Sigma-Aldrich, anhydrous, denatured), sodium hydroxide (Sigma-Aldrich, ACS reagent, ≥97.0%, pellets), hydrochloric acid (Sigma-Aldrich, ACS reagent, 37%), paraffin oil (Sigma-Aldrich, puriss., meets analytical specification of Ph. Eur., BP, viscous liquid), isopropyl palmitate (Sigma-Aldrich, technical grade, 90%), and sunflower oil (Supelco, analytical standard) were used as received. Dimethyl sulfoxide-d_6 (DMSO-d_6, Sigma-Aldrich, anhydrous, 99.9 atom % D) was used as deuterated solvents for NMR studies. 2-(Butylthiocarbonothioylthio)propanoate trithiocarbonate (MCEBTTC) was synthesized according to the procedure reported in the Supporting Information of this paper. 2,2′-[Carbonothioylbis(thio)]bis[2-methylpropanoic acid] (BDMAT) was synthesized as described in the literature.[63] *N*,*N*-Dimethyl lactamide acrylate (DMLA) and ethyl lactate acrylate (ELA) were synthesized according to the procedure reported in the literature using natural EL (98%, Merck) and AGNIQUE AND 3L (DML) kindly donated by BASF SE (Ludwigshafen, Germany).[20]

Characterization. ^{1}H NMR spectra were recorded on a Varian Mercury Plus 400 and 300 MHz spectrometers. Molecular weights (M_n number and M_w weight-average molecular weights) and dispersity ($Đ$) of the samples were determined by GPC using DMF (containing 0.01 M LiBr) as the eluent in a Viscotek GPCmax instrument equipped with a model 302 TDA detector based on refractive index and intrinsic viscosity and two columns (Agilent Technologies-PolarGel-L and M, 8 μm, 30 cm) at a flow rate of 1.0 mL min^{-1} and 50 °C. Narrow dispersity PMMA standards (Polymer Laboratories) were used to make a universal calibration curve. For sample preparation, the purified dry samples were dissolved in the eluent, filtered through a PTFE syringe filter (Minisart SRP 15, Sartorius stedim biotech, PTFE membrane filter; pore size, 0.2 μm; filter diameter, 15 mm), and analyzed by GPC. The collected spectra were analyzed with the use of an OmniSEC instrument (v5.0) (Malvern). Dynamic light scattering (DLS) measurements of the solution at different water concentrations were carried out using a Malvern Zetasizer Ultra instrument. Surface tension of water polymer solutions at different concentrations was measured with an OCA 15EC tensiometer from Dataphysics using the pendant drop method. The 633 nm (red light) photoreactor used in the present study was constructed on the basis of a similar one reported in the literature[64] using the SMD 3528 5050 5630 RGB LED strip light. The 5 m strip of 300 LEDS was wound on the inside of a 10 cm diameter aluminum jar with a hole in the base and the lid (Figure S1). The temperature was controlled using a water jacket equipped with a Julabo F12-ED thermos-controller. The measured irradiance of the LED results to be 13.8 W/m^2. The irradiance of the red light was measured at 638 nm (closest wavelength of the power meter available) using a ThorLabs S120C power meter equipped with a ThorLabs 400−1100 nm, 50 mW sensor. The morphology of the micelles was analyzed by transmission electron microscopy (TEM) and cryo-transmission electron microscopy (cryo-TEM) using an FEI Tecnai T20 operating at 200 keV. Images were recorded under low-dose conditions with a slow-scan CCD camera. For cryo-TEM, a few microliters of each sample solution were placed on mesh carbon-coated copper grids (Quantifoil 3.5/1, Quantifoil Micro Tools, Jena, Germany). Grids with sample were vitrified in liquid nitrogen (Vitrobot, FEI, Eindhoven, The Netherlands) and transferred to a FEI T20 cryo-electron microscope operating at 200 keV. Images were recorded on a slow scan CCD camera under low-dose conditions.

Synthesis of a Random Copolymer Poly(DMLA-*r*-ELA) via PET-RAFT. DMLA (1.5 g) and ELA (0.8 g) (molar ratio 2:1), MCEBTTC (0.04 g) as RAFT agent, DMSO (5.5 mL) as solvent, ZnTTP (366 μL of a stock solution in DMSO having a concentration of 3.8×10^{-5} M) as photocatalyst, and DMF (0.5 mL) as internal reference were added in a 20 mL vial. The vial was closed using a rubber septum. This solution was then degassed by argon bubbling for 30 min, and the reaction was started when the red light (~630 nm) was turned on. Aliquots of solution were taken at specific times to follow the kinetics and analyzed by ^{1}H NMR. The reaction was stopped once it reached high conversion values (≥90%) by switching off the light. The polymer solution was dialyzed against acetone, refreshing the solvent at least 3 times over a period of 2 days, using a membrane with a 1.0 kDa molecular weight cutoff value. The final polymer was recovered as yellowish solid by removing acetone using a vacuum oven over a period of 24 h.

Synthesis of Poly(DMLA) Macro-RAFT Agents. Mono- and difunctional poly(DMLA) macro-RAFT agents were synthesized via PET-RAFT and thermally initiated-RAFT polymerizations, respectively, according to the following procedures. In the case of thermally

https://doi.org/10.1021/acssuschemeng.2c04354
ACS Sustainable Chem. Eng. 2022, 10, 14806−14816

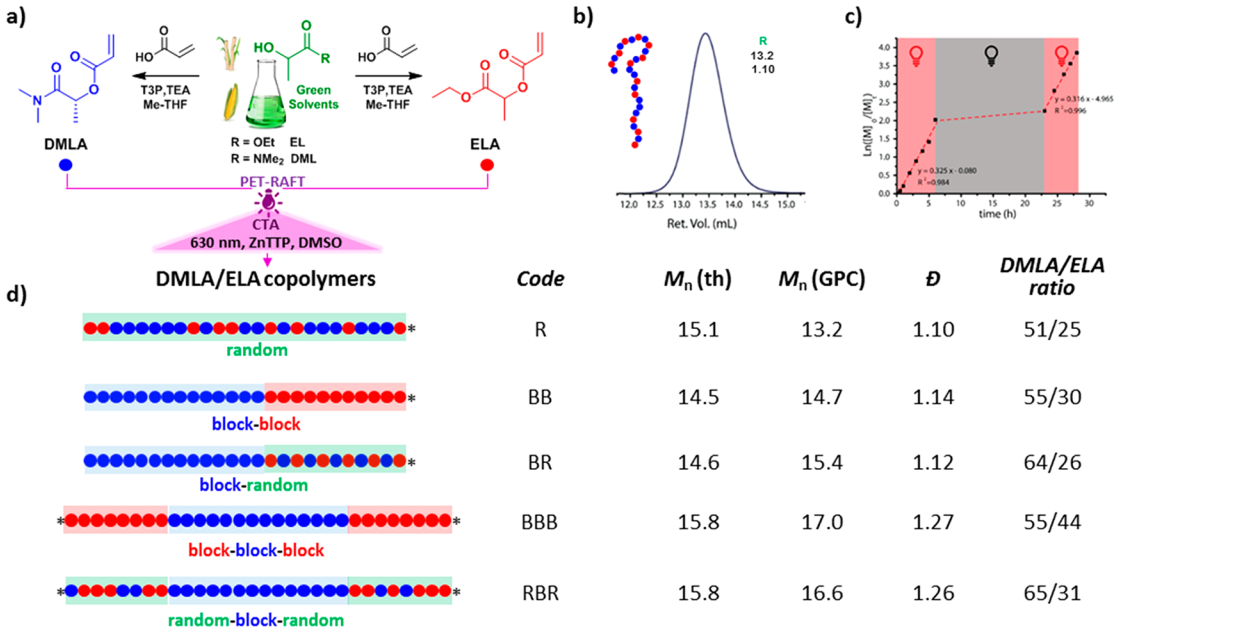

Figure 1. (a) Synthesis of DMLA and ELA acrylic monomers from the corresponding green solvents. (b) GPC trace of poly(DMLA-*r*-ELA) random copolymer **R**. Numbers shown together with the GPC trace correspond to M_n (GPC, kg/mol) and $Đ$. (c) Evolution of the $\ln([M]_0/[M])$ vs time for the ON−OFF−ON PET-RAFT random copolymerization of DMLA and ELA. (d) Schematic representation of the targeted composition profiles of DMLA/ELA copolymers together with the corresponding code, molar mass, and composition data for the synthesized copolymers. Additional molecular characterization is reported in Table S1.

initiated-RAFT polymerization, typically, DMLA (1.5 g), the RAFT agent BM1812 (0.08 g), anisole (5.5 mL), DMF (0.5 mL) as internal reference to track the monomer conversion via ^{1}H NMR, and AIBN (0.002 g) were added to a 20 mL vial. The vial was closed using a rubber septum. This solution was then degassed by argon bubbling for 30 min and heated to 65 °C. When PET-RAFT was used, the procedure was identical to the one just described, except the ZnTTP photocatalyst (366 μL of a photocatalyst stock solution in DMSO having a concentration of 3.8×10^{-5} M) instead of AIBN was added. In this case, after the addition, the vial was closed using a rubber septum and the solution was then degassed by argon bubbling for 30 min; the reaction was then started by turning the red light on (~630 nm). The kinetic analysis and work up were performed as described above. The final polymers were recovered as a yellowish solid by removing acetone using a vacuum oven over a period of 24 h.

Chain-Extension of Poly(DMLA) Macro-RAFT Agents. The chain extensions were performed via PET-RAFT polymerization as follows: poly(DMLA) Macro-RAFT agent (2.0 g) (monofunctional if the target polymer is a diblock copolymer or difunctional if it is a triblock), the monomer (1.0 g) (ELA if the desired block is PELA or a 3:1 mixture of ELA and DMLA if the desired block is poly(ELA-*r*-DMLA)), DMSO (6.5 mL) as solvent, DMF (0.5 mL) as internal reference, and ZnTTP photocatalyst were added to a 20 mL vial. The vial was closed using a rubber septum. This solution was then degassed by argon bubbling for 30 min, and the reaction was started when the red light (~630 nm) was turned on. The kinetic analysis and work up were performed as described above. The final polymers were recovered as yellowish solids by removing acetone using a vacuum oven over a period of 24 h.

RESULTS AND DISCUSSION

DMLA and ELA Synthesis from Green Lactic Acid-Based Solvents. Although EL and DML are chemicals with existing large volume uses as green solvents, their secondary hydroxyl functionality also enables their exploitation as precursors of reactive biobased (meth)acrylic monomers (Figure 1a).[19,20,40]

As reported in a previous publication,[19] EL solvent was converted into the corresponding acrylic derivative using a low environmental impact methodology that uses acrylic acid to introduce the reactive moiety and T3P as an ester-coupling promoter in the presence of TEA. Herein, this methodology was also adapted to synthesize the water-soluble DMLA monomer in 73% yield from the green solvent DML, which is marketed by BASF under the name Agnique AML 3L. In both cases, Me-THF was used as reaction media and chromatographic purification protocols were avoided to maximize the sustainability angle of the monomer synthesis step.

PET-RAFT to Produce ELA/DMLA Copolymers with Different Composition Profiles. Model lactic acid-derived (meth)acrylic block copolymers comprising two or more homopolymer segments were recently prepared using various reversible-deactivation radical polymerization (RDRP) methods.[19,20] Herein, five linear amphiphilic DMLA/ELA copolymers with comparable monomer composition (~65 mol % hydrophilic monomer) and number-average molar masses (M_n ~ 15 000 g·mol^{-1}) but different monomer distribution profiles were prepared using PET-RAFT polymerization activated by ZnTTP using a red light (633 nm). This RDRP method was preferred because it satisfies multiple principles of green chemistry, e.g., oxygen tolerance and room temperature polymerization, while minimizing the side reactions that usually are associated with poor control and poorly defined polymers.

First, a poly(DMLA-*r*-ELA) random copolymer precursor (**R**) was synthesized by PET-RAFT at room temperature using MCEBTTC as RAFT agent. The copolymerization using 150 ppm of ZnTTP at a DMLA/ELA molar feed ratio of 2.00 resulted in a monomodal polymer with low dispersity ($Đ$ = 1.10, Figure 1b) and experimental number-average molecular weight in good agreement with the theoretical value calculated from the monomer/CTA ratio and the monomer conversion (13 200 vs 15 100 g·mol^{-1}). Kinetic analysis revealed a linear increase of

https://doi.org/10.1021/acssuschemeng.2c04354
ACS Sustainable Chem. Eng. 2022, 10, 14806−14816

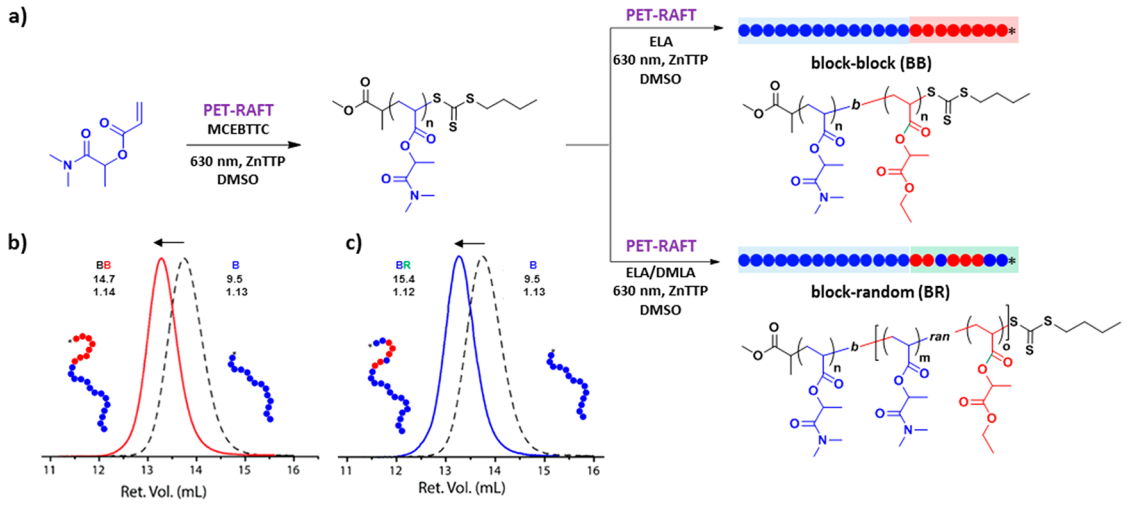

Figure 2. (a) Synthesis of DMLA/ELA copolymers **BB** and **BR** via PET-RAFT polymerization of ELA and ELA/DMLA, respectively, using a poly(DMLA) macroinitiator (M_n = 9500 g·mol^{-1}, $Đ$ = 1.13). (b) GPC traces of poly(DMLA) macroinitiator and **BB** copolymer. (c) GPC traces of poly(DMLA) macroinitiator and **BR** copolymer. Numbers shown together with the GPC traces correspond to M_n (GPC, kg/mol) and $Đ$.

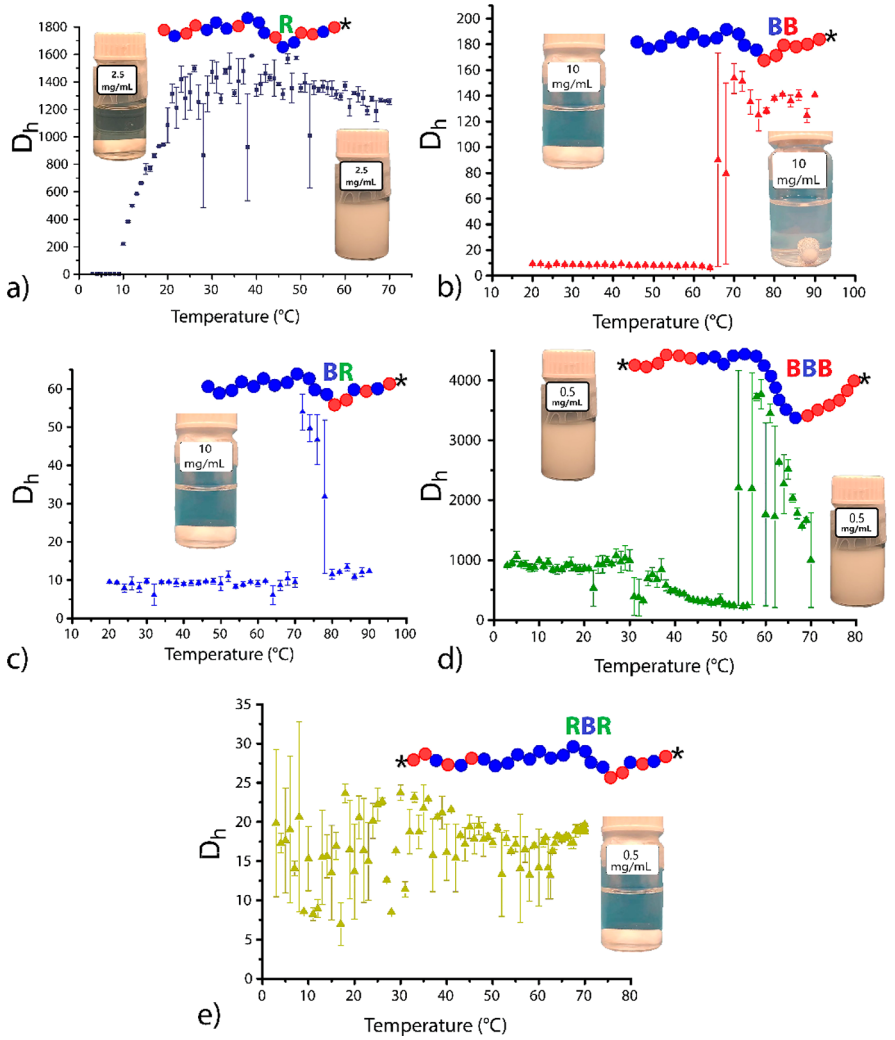

Figure 3. DLS hydrodynamic diameter as a function of temperature for the polymers synthesized in this work. In particular, (a) solution at 2.5 mg/mL of copolymer **R**, (b) solution at 10 mg/mL of copolymer **BB**, (c) solution at 10 mg/mL of copolymer **BR**, (d) solution at 0.5 mg/mL of copolymer **BBB**, and (e) solution at 0.5 mg/mL of copolymer **RBR**.

$\ln([M]_0/[M])$ with time, which is in agreement with a constant number of propagating chains throughout the polymerization (Figure 1c). Moreover, efficient temporal control of polymer chain growth was possible by ON−OFF light switching.

https://doi.org/10.1021/acssuschemeng.2c04354
ACS Sustainable Chem. Eng. 2022, 10, 14806−14816

Although, the overlapping of vinyl signals prevented the calculation of individual conversions by ^{1}H NMR analysis, the characteristic methine signals at ∼5.4 ppm for DMLA and ∼5.1 ppm for ELA allowed one to quantify the final ratio of 1.92 between the hydrophilic and hydrophobic monomers in the isolated copolymer **R**, which is close to the feed (2.00).

Next, a series of block copolymer precursors were synthesized applying the macroinitiator approach. The chemical route used for the synthesis of the copolymers **BB** and **BR** is depicted in Figure 2a. Briefly, a water-soluble DMLA homopolymer was synthesized by PET-RAFT using MCEBTTC as CTA and under identical conditions as described above for the preparation of the copolymer **R**, i.e., ZnTTP as photocatalyst and red light as the activator. The RAFT polymerization proceeded up to 91% conversion and afforded a monomodal poly(DMA) macroinitiator with molecular weight in close agreement with the theoretical value (9500 vs 11 800 g·mol^{-1}). The produced poly(DMLA) was isolated by dialysis and subsequently employed as macro-CTA to produce two AB copolymers with comparable molar mass but with differing composition profiles, poly(DMLA-*b*-ELA) (**BB**) and poly(DMLA-*b*-[DMLA-*r*-ELA]) (**BR**) (Figure 2a). Irrespective of the composition profile, the PET-RAFT polymerization proceeded with linear first-order kinetics, which can be regulated by ON−OFF light switching up to high conversion (>90%) (Figures S2 and S3). The successful formation of both copolymers was supported by a clear and symmetrical displacement of the GPC peak corresponding to the macro-CTA toward higher molecular weights after the chain extension (Figure 2b,c).

Subsequently, the same approach was used to access ABA triblock copolymer precursors with poly(DMLA) middle block and either homopolymer or mixed outer blocks (Figure 1b). In this case, BM1812 was used as CTA to produce a suitable and a well-defined telechelic poly(DMLA) macro-CTA (Figure S4). To solve solubility issues with BM1812, we resort to the use of thermo-initiated RAFT polymerization in anisole to produce the targeted bifunctional macroinitiator (M_n = 9500 g·mol^{-1}, $Đ$ = 1.30). ^{1}H NMR monitoring of the polymerization process showed that the integral of the proton signal associated with the terminal $-CH_3$ of the CTA Z-group at ∼0.9 ppm remained constant over time and up to high conversion, thus suggesting a high chain-end fidelity of the final polymer. Furthermore, the difunctional poly(DMLA) macro-CTA was chain extended via PET-RAFT at room temperature with ELA or a 3:1 mixture of DMLA and ELA to yield triblock copolymers poly(ELA-*b*-DMLA-*b*-ELA) (**BBB**) and poly[(DMLA-*r*-ELA)-*b*-DMLA-*b*-(DMLA-*r*-ELA)] (**RBR**), respectively. The formation of both macromolecular structures was demonstrated by the clear chain extensions observed by GPC leading to final triblock copolymers with narrow molecular weight distributions ($Đ$ = 1.27 for **BBB** and $Đ$ = 1.26 for **RBR**, respectively) (Figures S5 and S6). These results further demonstrate that PET-RAFT polymerization is a versatile tool for the production of different lactic acid-derived copolymers with comparable molar masses but differing composition profiles.

Self-Assembly and Thermoresponsive Behavior. The obtained series of polymers, consisting of linear structures with comparable molecular weights but completely different distribution of monomers, display distinct and interesting solution behavior. All investigated polymers are directly soluble in water giving a turbid or milky solution, typical of block copolymer assembly. It was also noticed that some of the polymers show temperature-dependent behavior in water, in particular the presence of a lower critical solution temperature (LCST).[62] For example, the solution of copolymer **R** is turbid at room temperature but becomes completely transparent by cooling to 4 °C

For this reason, a more detailed study was carried out by DLS. Low concentration aqueous solutions of the prepared polymers, in the range from 0.5 to 10 mg/mL, were analyzed by DLS as a function of the temperature in the range of 4−90 °C (Figure 3). The polymer concentration was optimized for each case, depending on visualization of the turbidity.

It has been previously shown that for some thermoresponsive polymers the LCST can be tuned by the polymer composition and architecture.[65−67] Also in our case, polymers with different architectures displayed different LCSTs and behaviors. In particular, the polymer with random structure **R** displayed a LCST of ∼17 °C, below which it is fully soluble (Figure 3a).

Conversely, the **BB** and **BBB** copolymers show turbidity and the presence of some aggregates also at low temperature (much more pronounced for **BBB**), but at their LCST (∼65 and ∼55 °C, respectively), the turbidity significantly increases, as well as the hydrodynamic diameter measured by DLS (Figure 3b,d), indicating the formation of new bigger aggregates. As the polymers were already forming aggregates at lower temperatures, these are not LCSTs in the proper sense, but we will stick to this nomenclature for lack of a better definition. The fact that **R** is the only fully soluble polymer at low temperature can be explained by the fact that all the other polymers have a blocky nature, where the hydrophobic block either is only constituted by ELA or is richer in it. This favors the formation of aggregates. The LCST does not seem to be dependent on polymer concentration (Figure S7); however, the cloud point temperature may be, as shown visually by Video S1. However, we did not perform a rigorous measurement of the latter.

It is noteworthy that the p(DMLA) structure is similar to that of other well-known thermoresponsive polymers, containing substituted amide groups (such as PNIPAM). However, it is interesting that, in the specific case of DMLA, the thermoresponsive behavior arises in combination with ELA, while polymers with long sequences of p(DMLA) do not show the same feature.

The self-assembly of a diblock copolymer P(DMLA-*b*-ELA) in water was previously reported in the literature,[20] but in that case, the thermoresponsive behavior was not investigated. Notably, in the mentioned previous work, the polymer could only be solubilized in water by transfer from a THF solution, and not directly, indicating that this step was necessary in order to achieve self-assembly. This can be ascribed to the fact that the hydrophobic block in the previous work had comparable length to the hydrophilic one, while in the present work it is significantly shorter, likely favoring spontaneous self-assembly by direct dissolution of the polymer in water. The dimensions of the aggregates were significantly different from that observed here with DLS (Figure 3), suggesting that the aggregation phenomena were complex and different for each polymer. The different size might be related to the different M_n (18 kDa of the previously reported polymer vs 14.5 kDa of the polymer synthesized in this work) and DMLA/ELA ratio (1 in the previously reported polymer vs 1.76 of the polymer synthesized in this work), but the data are insufficient to allow a clear correlation at this stage.

DLS of the triblock **BBB** showed some transition happening above its LCST. It must be noted here that, due to possible multiple scattering phenomena in turbid systems, the measured

https://doi.org/10.1021/acssuschemeng.2c04354
ACS Sustainable Chem. Eng. 2022, 10, 14806−14816

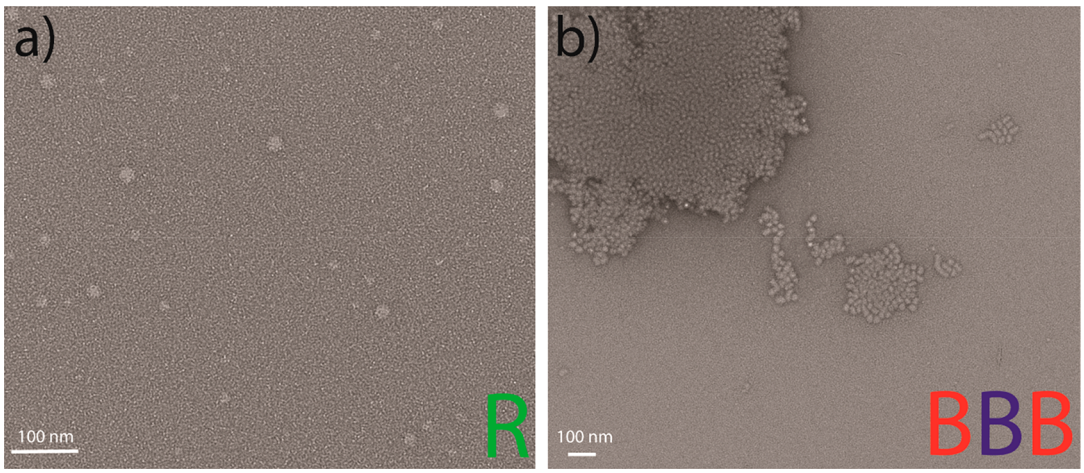

Figure 4. Negative staining TEM of the polymers synthesized in this work showing a thermoresponsive behavior. (a) **R** copolymer solution at 0.01 mg/mL and (b) **BBB** copolymer solution at 0.001 mg/mL.

Table 1. Summary of Polymer Solution Data

	R	BB	BBB	BR	RBR
appearance at low T	clear	slightly turbid	milky	slightly turbid	slightly turbid
LCST	17	65	55	none	none
D_h (DLS) below LCST	not detected	∼10 nm	∼1000 nm[a]	∼10 nm	∼20 nm
D_h (DLS) above LCST	>1200 nm	∼140 nm	2000−3000 nm[a]		
morphology of aggregates at 25 °C (TEM)	spherical micelles	not detected	connected micelles		

[a]Probably not accurate due to multiple scattering.

hydrodynamic diameters in this particular case are only indicative; however, changes in the correlation function and the particle count rate clearly indicate aggregation phenomena (see Figure S7). Those observations suggested that the triblock copolymer may form a network of connected micelles, as already reported in the literature for analogous systems.[68] From these observations, it was possible to conclude that the LCST depends more on the polymer architecture than on the DMLA/ELA ratio.

Analogous measurements were carried out on polymer solutions of the poly(DMLA) chain-extended with random−blocks (**BR** and **RBR**), but those copolymers did not display a LCST.

As their hydrophobic block is comparatively richer in ELA than **R**, one would expect to see further aggregation also in these cases; however, none is observed (Figure 3c,e). For **BR**, there seems to be a "jump" in particle size at high temperatures, but visually, no further aggregation could be observed.

This may signify that the aggregation process did not depend only on the hydrophobic block composition but also on the overall polymer structure and composition.

The three copolymers that displayed thermoresponsive behavior (**R**, **BB**, and **BBB**) were analyzed by cryo-TEM and TEM to gain more information on the kind of aggregates formed.

Despite the observation of a clear formation of aggregates for **R** solution at 0.01 mg/mL, cryo-TEM was not able to detect them when the sample was prepared at either 10 or 25 °C. Negative staining TEM was carried out on the same solution, drying the grid with an IR lamp (∼30−35 °C). In this case, TEM showed the presence of spherical aggregates ($r \sim 25$ nm) (Figure 4a), confirming that above the LCST the polymer was able to self-assemble into micelles. **BB** solutions did not show visible aggregates at the TEM. More interesting were the results of the triblock polymer solution (**BBB** at 0.01 mg/mL) analyzed by TEM. The solution was turbid at 25 °C, and according to the DLS data, the aggregates were big enough to suggest the presence of a connected-micelle network typical of triblock copolymer assembly. Indeed, at 25 °C, the TEM (Figure 4b) showed the presence of numerous micelles ($r \sim 20$ nm) connected to each other forming macroaggregates up to 800 nm, in line with the DLS data. It can be noted here that TEM was measured at lower concentrations than DLS due to specific instrument requirements. However, as these polymers should give kinetically "frozen" micellar aggregates, the concentration should not have a significant effect. What happened at 65 °C could be a transition to a different kind of aggregate (such as worm-like micelles),[69,70] but this should be further investigated. Data about self-assembly, thermoresponsive behavior, and morphology of the studied polymers are summarized in Table 1.

Surface Tension and Preliminary Emulsion Studies with Different Oils. Given the possible application of such biobased polymers as emulsifiers and/or emulsion stabilizers, we further investigated polymer solutions from the point of view of surface tension and emulsion stabilization of various oils. Comparing the different surface tension values as a function of the polymer concentration, no big difference was observed between polymers having the diblock and triblock architecture (Figure 5). It is worth mentioning that measurements of the triblock with mixed outer segments (**RBR**) using the pendant drop method resulted in a particular challenge due to poor stability of the forming drop. The random copolymer **R** is remarkably more surface active, as shown in Figure 5, displaying a decrease of the surface tension up to 42 mN/m already at low polymer concentration values. These results are in line with that reported in the literature about the effect of the polymer

https://doi.org/10.1021/acssuschemeng.2c04354
ACS Sustainable Chem. Eng. 2022, 10, 14806−14816

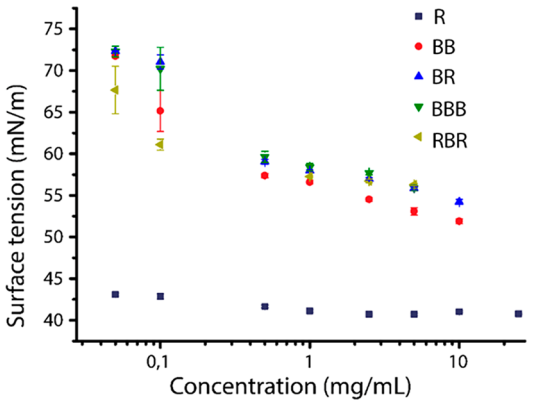

Figure 5. Comparison of surface tension as a function of the polymer concentration for the different polymer architectures.

architecture (random vs block copolymers) on surface tension.[53]

As anticipated, we also carried out preliminary tests aimed at evaluating how the prepared polymers behave as emulsion stabilizers with three oils with different polarities (paraffin oil, isopropyl palmitate oil, and sunflower oil). For this reason, equal volumes of oil and aqueous polymer solutions at 5 mg/mL were put in contact in a graduated test tube and shaken vigorously, and emulsion formation was observed. As reported in the literature, it is expected that oil polarity and the chemical nature of the emulsifier affect the emulsion type, droplet size, and stability of the emulsions.[71,72]

The stability over time was monitored by measuring the volume of the emulsified phase until equilibrium (Figures S8–S10).

In all cases, the bottom layer (water) remained transparent (Figures S8–S10), indicating that water/oil emulsions are formed, rather than o/w. For all the oils, the triblock copolymers proved to be the most efficient stabilizers, stabilizing up to 40% (v/v) of the water in the oil phase (Figure 6). In all cases, a partial precipitation of the polymer (as confirmed by ^{1}H NMR, Figure S11) was observed after several hours, which did not affect the stability of the emulsion.

Overall, no clear trend could be identified with respect to the polymer architecture and type of oil. The random copolymer was less effective in stabilizing paraffin and sunflower oil emulsions compared to the other polymers, but it proved to be the best stabilizer for isopropyl palmitate. The diblock copolymers were less effective with isopropyl palmitate oil emulsion but proved to be good emulsifiers in the other cases. We can only conclude that many factors are at play at the same time (hydrophobic/hydrophilic balance, hydrogen bonding, distribution of hydrophobic groups, dynamics of the system), making it difficult to find trends.

Given the thermoresponsive aggregation behavior, we also preliminarily investigated the effect of temperature on emulsion stabilization. The random copolymer (**R**) was the only one used for this study. It showed better stabilization of paraffin oil

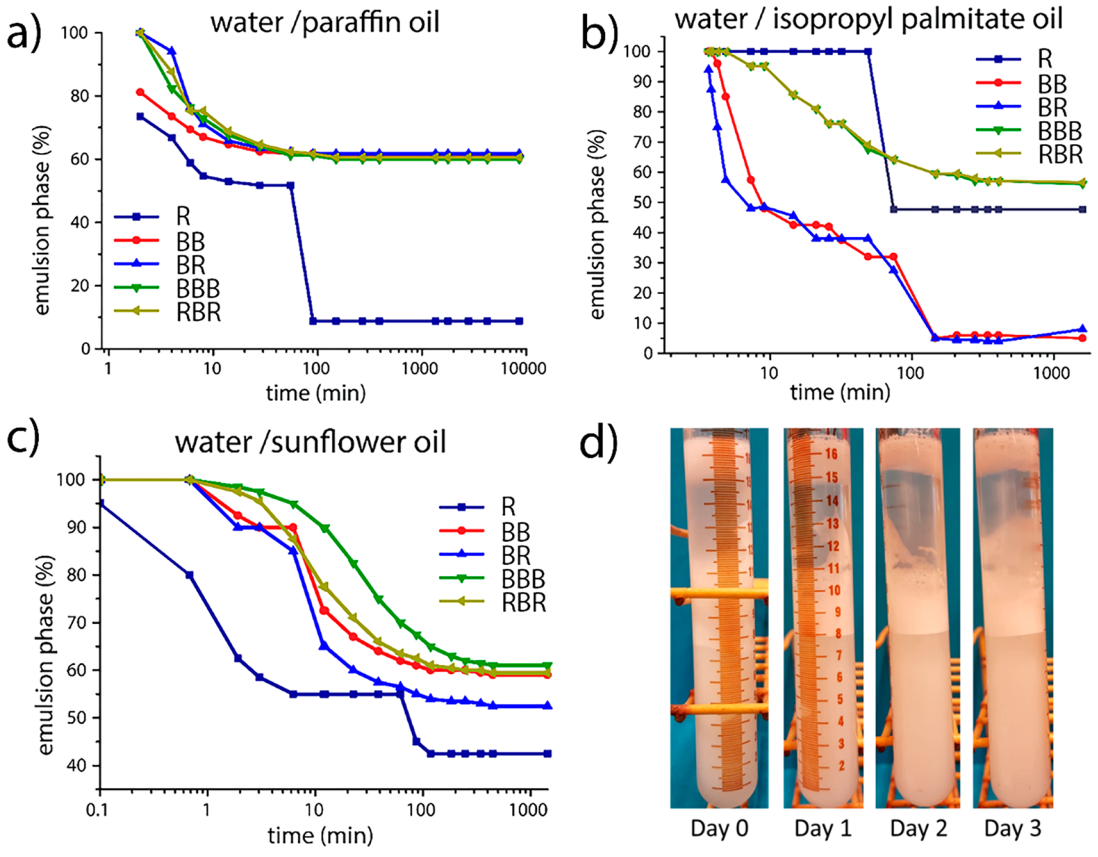

Figure 6. Comparison of the kinetic study of (a) the emulsion stability over time of the 50% v/v water/paraffin oil stabilized by 0.25% w/v of polymer; (b) the emulsion stability over time of the 50% v/v water/isopropyl palmitate oil stabilized by 0.25% w/v of polymer; (c) the emulsion stability over time of the 50% v/v water/sun flower oil stabilized by 0.25% w/v of polymer. (d) Images of the kinetic study of the water/paraffin oil emulsions stabilized by copolymer **R** at 4 °C.

https://doi.org/10.1021/acssuschemeng.2c04354
ACS Sustainable Chem. Eng. 2022, 10, 14806−14816

emulsions at low temperature (4 °C) compared to room temperature (Figure 6d). Moreover, in this case, the bottom water phase appeared cloudy and not transparent as opposed to the same emulsion at room temperature, suggesting the presence of polymer aggregates in water. No clear correlation between oil polarity, polymer structure, and emulsion stability was found. We can conclude that the prepared polymers are effective stabilizers of w/o emulsions and the best polymer was dependent on the type of oil used to prepare the emulsion, probably due to the different polarities. It is noteworthy that, although being 2/3 composed of the hydrophilic monomer, this polymeric surfactant promoted the formation of w/o emulsions, apparently contradicting the Bancroft rule. This shows that polymeric surfactants may have different dynamics than low molecular weight ones.

CONCLUSIONS

In this work, we reported the synthesis, characterization, and solution properties of thermoresponsive lactic acid-derived polymeric surfactants characterized by different molecular architectures. The use of two bioderived monomers such as DMLA and ELA for the preparation of amphiphilic polymers represent an advantage over other acrylic monomers in terms of sustainability and green chemistry principles. To synthesize polymers characterized by different architectures, PET-RAFT activated by ZnTTP photocatalyst was used as a synthetic strategy. The use of red light (633 nm) to initiate polymerization unifies multiple aspects of green chemistry and minimizes possible side reactions that usually lead to poor control and poorly defined polymers in photoinitiated processes.[59] Moreover, the use of a photochemistry-based method provides the basis for polymeric materials manufacturing via 3D printing techniques.

After preparing five copolymers with different monomer distributions, we focused our attention on studying the solution behavior of the prepared polymers in water solution. Some of them were identified to be thermoresponsive, showing a LCST in the range of 13−70 °C, depending on the molecular architecture. Specifically, as confirmed first by DLS and then by TEM, a random copolymer of DMLA and ELA (51:25) is fully soluble at low temperatures and able to assemble into spherical micelles above 17 °C. A thermoresponsive behavior was also shown by the corresponding diblock copolymer, but in this case, the polymer already aggregates at low temperature; further aggregation was observed above 65 °C. The triblock copolymer aggregates showed a significant difference in morphology, since the presence of connected micelles was already shown at low temperature, and even larger structures seemed to form according to DLS at 55 °C. For the random−blocks, no transitions were observed at any investigated temperature. This suggests that the DMLA/ELA ratio in the hydrophobic block may not be a determining factor of this associative behavior, but rather, it is due to the overall composition of the polymer.

In terms of surface activity, the random copolymer showed significantly lower surface tension than the block copolymers. Preliminary tests aimed at evaluating the prepared copolymers as emulsion stabilizers showed that they all form w/o emulsions with three oils characterized by different polarities with no apparent correlation with the polymer structure. Notably, the kind of emulsions formed are w/o, despite the polymers being 2/3 constituted by the hydrophilic monomer, apparently contradicting the Bancroft rule. This goes to show the complexity of polymeric surfactants compared to low-molecular ones. The triblock copolymers were the most efficient stabilizers, despite the minimal surface activity, while diblock and random copolymer effectiveness seemed to be dependent on the type of oil used.

The results obtained in this work are promising for a future development of bioderived polymeric surfactants for industrial applications. Further studies on the molecular weight effect and different DMLA/ELA ratios can help to better understand how to engineer the polymer composition in order to achieve the desired final solution properties.

ASSOCIATED CONTENT

Supporting Information

The Supporting Information is available free of charge at https://pubs.acs.org/doi/10.1021/acssuschemeng.2c04354.

Synthetic procedure for RAFT agent, pictures of apparatus used, H^1-NMR spectra, GPC traces, DLS data, and emulsion pictures (PDF)

Video showing **R** polymer solutions at various concentrations from 4 °C to room temperature (MP4)

AUTHOR INFORMATION

Corresponding Author

Patrizio Raffa − *Smart and Sustainable Polymeric Products, Engineering and Technology Institute Groningen, University of Groningen, 9747 AG Groningen, The Netherlands;* orcid.org/0000-0003-0738-3393; Email: p.raffa@rug.nl

Authors

Nicola Migliore − *Smart and Sustainable Polymeric Products, Engineering and Technology Institute Groningen, University of Groningen, 9747 AG Groningen, The Netherlands; Empa, Swiss Federal Laboratories for Materials Science and Technology, Laboratory for Biomimetic Membranes and Textiles, CH-9014 St. Gallen, Switzerland*

Aleksander Guzik − *Smart and Sustainable Polymeric Products, Engineering and Technology Institute Groningen, University of Groningen, 9747 AG Groningen, The Netherlands;* orcid.org/0000-0003-1184-9176

Marc C. A. Stuart − *Electron Microscopy, Groningen Biomolecular Sciences and Biotechnology Institute, University of Groningen, 9747 AG Groningen, The Netherlands;* orcid.org/0000-0003-0667-6338

Marc Palà − *Laboratory of Sustainable Polymers, Department of Analytical Chemistry and Organic Chemistry, University Rovira i Virgili, 43007 Tarragona, Spain*

Adrian Moreno − *Laboratory of Sustainable Polymers, Department of Analytical Chemistry and Organic Chemistry, University Rovira i Virgili, 43007 Tarragona, Spain*

Gerard Lligadas − *Laboratory of Sustainable Polymers, Department of Analytical Chemistry and Organic Chemistry, University Rovira i Virgili, 43007 Tarragona, Spain;* orcid.org/0000-0002-8519-1840

Complete contact information is available at: https://pubs.acs.org/10.1021/acssuschemeng.2c04354

Author Contributions

N.M.: conceptualization, data curation, formal analysis, investigation, methodology, visualization, writing−original draft; A.G.: investigation and formal analysis of part of the emulsion studies; M.A.C.S.: TEM analysis; G.L.: monomer

synthesis review and editing; M.P.: monomer synthesis review and editing; A.M.: monomer synthesis review and editing; P.R.: conceptualization, methodology, project administration, supervision (lead), writing—reviewing and editing. All authors have given approval to the final version of the manuscript.

Notes

The authors declare no competing financial interest.

■ ACKNOWLEDGMENTS

Funding from MCIN/AEI/10.13039/501100011033 through grant PID2020-114098RB-100 (to G.L.) and the Serra Hunter Programme of the Government of Catalonia (to G.L.) is gratefully acknowledged. M.P. thanks MICIN for FPI grant PRE2021-100387.

■ ABBREVIATIONS

DMLA, *N*,*N*-dimethyl lactamide acrylate; ELA, ethyl lactate acrylate; LA, lactic acid; PLA, poly(lactic acid); EL, ethyl lactate; DML, *N*,*N*-dimethyl lactamide; FRP, free radical polymerization; RDRP, reversible deactivation radical polymerization; LCST, lower critical solution temperature; UCST, upper critical solution temperature; T_{CP}, cloud point temperature; RAFT, reversible addition−fragmentation chain transfer; ATRP, atom transfer radical polymerization (ATRP); PET-RAFT, photoinduced electron/energy transfer-reversible addition−fragmentation chain transfer; SET-LRP, single electron transfer-living radical polymerization; CTA, chain transfer agent; GPC, gel permeation chromatography; H^1-NMR, proton nuclear magnetic resonance; DLS, dynamic light scattering; MCEBTTC, 2-(butylthiocarbonothioylthio)propanoate trithiocarbonate; BDMAT, 2′-[carbonothioylbis (thio)]bis[2-methylpropanoic acid]; BM1812, 1,4-phenylenebis(methylene) didodecyl dicarbonotrithioate; ZnTTP, 5,10,15,20-tetraphenyl-21*H*,23*H*-porphine zinc; AIBN, 2,2′-azobis(2-methylpropionitrile); DMF, *N*,*N*-dimethylformamide; DMSO-d_6, dimethyl sulfoxide-d_6; *Đ*, dispersity; TEM, transmission electron microscopy; cryo-TEM, cryo-transmission electron microscopy; THF, tetrahydrofuran; M_n, molecular weight

■ REFERENCES

(1) Zhang, C.; Xue, J.; Yang, X.; Ke, Y.; Ou, R.; Wang, Y.; Madbouly, S. A.; Wang, Q. From Plant Phenols to Novel Bio-Based Polymers. *Prog. Polym. Sci.* **2022**, *125*, 101473.

(2) Thakur, S.; Chaudhary, J.; Singh, P.; Alsanie, W. F.; Grammatikos, S. A.; Thakur, V. K. Synthesis of Bio-Based Monomers and Polymers Using Microbes for a Sustainable Bioeconomy. *Bioresour. Technol.* **2022**, *344*, 126156.

(3) Ma, Y.; Xiao, Y.; Zhao, Y.; Bei, Y.; Hu, L.; Zhou, Y. Biomass Based Polyols and Biomass Based Polyurethane Materials as a Route towards Sustainability. *React. Funct. Polym.* **2022**, *175*, 105285.

(4) Migliore, N.; Zijlstra, D. S.; Van Kooten, T. G.; Deuss, P. J.; Raffa, P. Amphiphilic Copolymers Derived from Butanosolv Lignin and Acrylamide: Synthesis, Properties in Water Solution, and Potential Applications. *ACS Appl. Polym. Mater.* **2020**, *2* (12), 5705−5715.

(5) Fan, Y.; Migliore, N.; Raffa, P.; Bose, R. K.; Picchioni, F. Synthesis of Zwitterionic Copolymers via Copper-Mediated Aqueous Living Radical Grafting Polymerization on Starch. *Polymers* **2019**, *11* (2), 192.

(6) Siyamak, S.; Laycock, B.; Luckman, P. Synthesis of Starch Graft-Copolymers via Reactive Extrusion: Process Development and Structural Analysis. *Carbohydr. Polym.* **2020**, *227*, 115066.

(7) Cazotti, J. C.; Fritz, A. T.; Garcia-Valdez, O.; Smeets, N. M. B.; Dubé, M. A.; Cunningham, M. F. Graft Modification of Starch Nanoparticles Using Nitroxide-Mediated Polymerization and the Grafting from Approach. *Carbohydr. Polym.* **2020**, *228*, 115384.

(8) Perkins, K. M.; Gupta, C.; Charleson, E. N.; Washburn, N. R. Surfactant Properties of PEGylated Lignins: Anomalous Interfacial Activities at Low Grafting Density. *Colloids Surf. A Physicochem. Eng. Asp.* **2017**, *530*, 200−208.

(9) Laurichesse, S.; Avérous, L. Chemical Modification of Lignins: Towards Biobased Polymers. *Prog. Polym. Sci.* **2014**, *39* (7), 1266−1290.

(10) Galbis, J. A.; García-Martín, M. D. G.; De Paz, M. V.; Galbis, E. Synthetic Polymers from Sugar-Based Monomers. *Chem. Rev.* **2016**, *116* (3), 1600−1636.

(11) Hojabri, L.; Kong, X.; Narine, S. S. Fatty Acid-Derived Diisocyanate and Biobased Polyurethane Produced from Vegetable Oil: Synthesis, Polymerization, and Characterization. *Biomacromolecules* **2009**, *10* (4), 884−891.

(12) Gandini, A.; Lacerda, T. M.; Carvalho, A. J. F.; Trovatti, E. Progress of Polymers from Renewable Resources: Furans, Vegetable Oils, and Polysaccharides. *Chem. Rev.* **2016**, *116* (3), 1637−1669.

(13) Noppalit, S.; Simula, A.; Billon, L.; Asua, J. M. On the Nitroxide Mediated Polymerization of Methacrylates Derived from Bio-Sourced Terpenes in Miniemulsion, a Step towards Sustainable Products. *Polym. Chem.* **2020**, *11*, 1151−1160.

(14) Bao, C.; Xu, X.; Chen, J.; Zhang, Q. Synthesis of Biodegradable Protein-Poly(ϵ-Caprolactone) Conjugates: Via Enzymatic Ring Opening Polymerization. *Polym. Chem.* **2020**, *11*, 682−686.

(15) Hatton, F. L. Recent Advances in RAFT Polymerization of Monomers Derived from Renewable Resources. *Polym. Chem.* **2020**, *11*, 220−229.

(16) Hermens, J. G. H.; Freese, T.; Van den Berg, K. J.; Van Gemert, R.; Feringa, B. L. A Coating from Nature. *Sci. Adv.* **2020**, *6* (51), 1−11.

(17) Adharis, A.; Ketelaar, T.; Komarudin, A. G.; Loos, K. Synthesis and Self-Assembly of Double-Hydrophilic and Amphiphilic Block Glycopolymers. *Biomacromolecules* **2019**, *20*, 1325−1333.

(18) Birajdar, M. S.; Joo, H.; Koh, W. G.; Park, H. Natural Bio-Based Monomers for Biomedical Applications: A Review. *Biomater. Res.* **2021**, *25* (1), 1−14.

(19) Bensabeh, N.; Jiménez-Alesanco, A.; Liblikas, I.; Ronda, J. C.; Cádiz, V.; Galià, M.; Vares, L.; Abián, O.; Lligadas, G. Biosourced All-Acrylic ABA Block Copolymers with Lactic Acid-Based Soft Phase. *Molecules* **2020**, *25* (23), 5740.

(20) Bensabeh, N.; Moreno, A.; Roig, A.; Rahimzadeh, M.; Rahimi, K.; Ronda, J. C.; Cádiz, V.; Galià, M.; Percec, V.; Rodriguez-Emmenegger, C.; Lligadas, G. Photoinduced Upgrading of Lactic Acid-Based Solvents to Block Copolymer Surfactants. *ACS Sustain. Chem. Eng.* **2020**, *8* (2), 1276−1284.

(21) Veith, C.; Diot-Néant, F.; Miller, S. A.; Allais, F. Synthesis and Polymerization of Bio-Based Acrylates: A Review. *Polym. Chem.* **2020**, *11*, 7452−7470.

(22) Liang, B.; Zhao, J.; Li, G.; Huang, Y.; Yang, Z.; Yuan, T. Facile Synthesis and Characterization of Novel Multi-Functional Bio-Based Acrylate Prepolymers Derived from Tung Oil and Its Application in UV-Curable Coatings. *Ind. Crops Prod.* **2019**, *138*, 111585.

(23) Quintens, G.; Vrijsen, J. H.; Adriaensens, P.; Vanderzande, D.; Junkers, T. Muconic Acid Esters as Bio-Based Acrylate Mimics. *Polym. Chem.* **2019**, *10*, 5555−5563.

(24) Makshina, E. V.; Canadell, J.; van Krieken, J.; Peeters, E.; Dusselier, M.; Sels, B. F. Bio-Acrylates Production: Recent Catalytic Advances and Perspectives of the Use of Lactic Acid and Their Derivates. *ChemCatChem.* **2019**, *11*, 180−201.

(25) Fouilloux, H.; Thomas, C. M. Production and Polymerization of Biobased Acrylates and Analogs. *Macromol. Rapid Commun.* **2021**, *42*, 2000530.

(26) Mora-Villalobos, J. A.; Montero-Zamora, J.; Barboza, N.; Rojas-Garbanzo, C.; Usaga, J.; Redondo-Solano, M.; Schroedter, L.; Olszewska-Widdrat, A.; Lopez-Gomez, J. P. Multi-Product Lactic Acid Bacteria Fermentations. *Fermentation* **2020**, *6* (1), 23.

(27) Ahmad, A.; Banat, F.; Taher, H. A Review on the Lactic Acid Fermentation from Low-Cost Renewable Materials: Recent Developments and Challenges. *Environ. Technol. Innov.* **2020**, *20*, 101138.

(28) Liu, X.; Zhang, Q.; Wang, R.; Li, H. Sustainable Conversion of Biomass-Derived Carbohydrates into Lactic Acid Using Heterogeneous Catalysts. *Curr. Green Chem.* **2020**, *7* (3), 282−289.
(29) Li, T.; Tang, Z.; Wei, H.; Tan, Z.; Liu, P.; Li, J.; Zheng, Y.; Lin, J.; Liu, W.; Jiang, H.; Liu, H.; Zhu, L.; Ma, Y. Totally Atom-Economical Synthesis of Lactic Acid from Formaldehyde: Combined Bio-Carboligation and Chemo-Rearrangement without the Isolation of Intermediates. *Green Chem.* **2020**, *22*, 6809−6814.
(30) Kim, K. H.; Kim, C. S.; Wang, Y.; Yoo, C. G. Integrated Process for the Production of Lactic Acid from Lignocellulosic Biomass: From Biomass Fractionation and Characterization to Chemocatalytic Conversion with Lanthanum(III) Triflate. *Ind. Eng. Chem. Res.* **2020**, *59* (23), 10832−10839.
(31) Ncube, L. K.; Ude, A. U.; Ogunmuyiwa, E. N.; Zulkifli, R.; Beas, I. N. Environmental Impact of Food Packaging Materials: A Review of Contemporary Development from Conventional Plastics to Polylactic Acid Based Materials. *Materials* **2020**, *13* (21), 4994.
(32) Khosravi, A.; Fereidoon, A.; Khorasani, M. M.; Naderi, G.; Ganjali, M. R.; Zarrintaj, P.; Saeb, M. R.; Gutiérrez, T. J. Soft and Hard Sections from Cellulose-Reinforced Poly(Lactic Acid)-Based Food Packaging Films: A Critical Review. *Food Packag. Shelf Life* **2020**, *23*, 100429.
(33) Abu Hajleh, M. N.; AL-Samydai, A.; Al-Dujaili, E. A. S. Nano, Micro Particulate and Cosmetic Delivery Systems of Polylactic Acid: A Mini Review. *J. Cosmet. Dermatol.* **2020**, *19*, 2805−2811.
(34) Liu, S.; Qin, S.; He, M.; Zhou, D.; Qin, Q.; Wang, H. Current Applications of Poly(Lactic Acid) Composites in Tissue Engineering and Drug Delivery. *Compos. Part B Eng.* **2020**, *199*, 108238.
(35) Ilyas, R. A.; Sapuan, S. M.; Harussani, M. M.; Hakimi, M. Y. A. Y.; Haziq, M. Z. M.; Atikah, M. S. N.; Asyraf, M. R. M.; Ishak, M. R.; Razman, M. R.; Nurazzi, N. M.; Norrrahim, M. N. F.; Abral, H.; Asrofi, M. Polylactic Acid (PLA) Biocomposite: Processing, Additive Manufacturing and Advanced Applications. *Polymers* **2021**, *13* (8), 1326.
(36) Di Lorenzo, M. L.; Androsch, R.*Industrial Applications of Poly (Lactic Acid)*; Springer, 2018; DOI: 10.1007/978-3-319-75459-8.
(37) Hatti-Kaul, R.; Chen, L.; Dishisha, T.; Enshasy, H. El. Lactic Acid Bacteria: From Starter Cultures to Producers of Chemicals. *FEMS Microbiol. Lett.* **2018**, *365* (20), 1−20.
(38) Purushothaman, M.; Krishnan, P. S. G.; Nayak, S. K. Effect of Nano Sepiolite Fiber on the Properties of Poly(Ethyl Lactate Acrylate): Hydrophilicity and Thermal Stability. *Mater. Focus* **2018**, *7* (1), 101−107.
(39) Purushothaman, M.; Krishnan, P. S. G.; Nayak, S. K. Poly(Alkyl Lactate Acrylate)s Having Tunable Hydrophilicity. *J. Appl. Polym. Sci.* **2014**, *131* (21), 40962.
(40) Moreno, A.; Bensabeh, N.; Parve, J.; Ronda, J. C.; Cádiz, V.; Galià, M.; Vares, L.; Lligadas, G.; Percec, V. SET-LRP of Bio- and Petroleum-Sourced Methacrylates in Aqueous Alcoholic Mixtures. *Biomacromolecules* **2019**, *20*, 1816−1827.
(41) Li, L.; Raghupathi, K.; Song, C.; Prasad, P.; Thayumanavan, S. Self-Assembly of Random Copolymers. *Chem. Commun.* **2014**, *50*, 13417−13432.
(42) Raffa, P.; Stuart, M. C. A.; Broekhuis, A. A.; Picchioni, F. The Effect of Hydrophilic and Hydrophobic Block Length on the Rheology of Amphiphilic Diblock Polystyrene-b-Poly(Sodium Methacrylate) Copolymers Prepared by ATRP. *J. Colloid Interface Sci.* **2014**, *428*, 152−161.
(43) Alexandridis, P. Amphiphilic Copolymers and Their Applications. *Curr. Opin. Colloid Interface Sci.* **1996**, *1* (4), 490−501.
(44) Guo, P.; Guan, W.; Liang, L.; Yao, P. Self-Assembly of pH-Sensitive Random Copolymers: Poly(styrene-co-4-vinylpyridine). *J. Colloid Interface Sci.* **2008**, *323* (2), 229−234.
(45) Imai, S.; Hirai, Y.; Nagao, C.; Sawamoto, M.; Terashima, T. Programmed Self-Assembly Systems of Amphiphilic Random Copolymers into Size-Controlled and Thermoresponsive Micelles in Water. *Macromolecules* **2018**, *51* (2), 398−409.
(46) Raffa, P.; Wever, D. A. Z.; Picchioni, F.; Broekhuis, A. A. Polymeric Surfactants: Synthesis, Properties, and Links to Applications. *Chem. Rev.* **2015**, *115* (16), 8504−8563.
(47) Letchford, K.; Burt, H. A Review of the Formation and Classification of Amphiphilic Block Copolymer Nanoparticulate Structures: Micelles, Nanospheres, Nanocapsules and Polymersomes. *Eur. J. Pharm. Biopharm.* **2007**, *65* (3), 259−269.
(48) Adams, M. L.; Lavasanifar, A.; Kwon, G. S. Amphiphilic Block Copolymers for Drug Delivery. *J. Pharm. Sci.* **2003**, *92* (7), 1343−1355.
(49) Farias, C. B. B.; Almeida, F. C.G.; Silva, I. A.; Souza, T. C.; Meira, H. M.; Soares da Silva, R. d. C. F.; Luna, J. M.; Santos, V. A.; Converti, A.; Banat, I. M.; Sarubbo, L. A. Production of Green Surfactants : Market Prospects. *Electron. J. Biotechnol.* **2021**, *51*, 28−39.
(50) Deljooei, M.; Zargar, G.; Nooripoor, V.; Takassi, M. A.; Esfandiarian, A. Novel Green Surfactant Made from L-Aspartic Acid as Enhancer of Oil Production from Sandstone Reservoirs : Wettability, IFT, Microfluidic, and Core flooding Assessments. *J. Mol. Liq.* **2021**, *323*, 115037.
(51) Hunter, S. J.; Armes, S. P. Pickering Emulsifiers Based on Block Copolymer Nanoparticles Prepared by Polymerization-Induced Self-Assembly. *Langmuir* **2020**, *36* (51), 15463−15484.
(52) Ward, M. A.; Georgiou, T. K. Thermoresponsive Polymers for Biomedical Applications. *Polymers* **2011**, *3* (3), 1215−1242.
(53) Migliore, N.; Picchioni, F.; Raffa, P. The Effect of Macromolecular Structure on the Rheology and Surface Properties of Amphiphilic Random Polystyrene-r-Poly(Meth)Acrylate Copolymers Prepared by RDRP. *Soft Matter* **2020**, *16*, 2836−2846.
(54) Zhang, J.; Farias-Mancilla, B.; Kulai, I.; Hoeppener, S.; Lonetti, B.; Prevost, S.; Ulbrich, J.; Destarac, M.; Colombani, O.; Schubert, U. S.; Guerrero-Sanchez, C.; Harrisson, S. Effect of Hydrophilic Monomer Distribution on Self-Assembly of a pH- Responsive Copolymer : Spheres, Worms and Vesicles from a Single Copolymer Composition. *Angew. Chem., Int. Ed.* **2021**, *60*, 4925−4930.
(55) Goswami, K. G.; Mete, S.; Chaudhury, S. S.; Sar, P.; Ksendzov, E.; Mukhopadhyay, C. D.; Kostjuk, S. V.; De, P. Self-Assembly of Amphiphilic Copolymers with Sequence-Controlled Alternating Hydrophilic−Hydrophobic Pendant Side Chains. *ACS Appl. Polym. Mater.* **2020**, *2* (5), 2035−2045.
(56) Armes, S. P.; Perrier, S.; Zetterlund, P. B. Introduction to Polymerisation-Induced Self-Assembly. *Polym. Chem.* **2021**, *12*, 8−11.
(57) Boyer, C.; Bulmus, V.; Davis, T. P.; Ladmiral, V.; Liu, J.; Perrier, S. Bioapplications of RAFT Polymerization. *Chem. Rev.* **2009**, *109* (11), 5402−5436.
(58) Perrier, S. 50th Anniversary Perspective: RAFT Polymerization - A User Guide. *Macromolecules* **2017**, *50* (19), 7433−7447.
(59) Corrigan, N.; Jung, K.; Moad, G.; Hawker, C. J.; Matyjaszewski, K.; Boyer, C. Reversible-Deactivation Radical Polymerization (Controlled/Living Radical Polymerization): From Discovery to Materials Design and Applications. *Prog. Polym. Sci.* **2020**, *111*, 101311.
(60) Liang, X.; Liu, F.; Kozlovskaya, V.; Palchak, Z.; Kharlampieva, E. Thermoresponsive Micelles from Double LCST-Poly(3-Methyl-N-Vinylcaprolactam) Block Copolymers for Cancer Therapy. *ACS Macro Lett.* **2015**, *4* (3), 308−311.
(61) Lutz, J. F.; Akdemir, Ö.; Hoth, A. Point by Point Comparison of Two Thermosensitive Polymers Exhibiting a Similar LCST: Is the Age of Poly(NIPAM) Over? *J. Am. Chem. Soc.* **2006**, *128* (40), 13046−13047.
(62) Roy, D.; Brooks, W. L. A.; Sumerlin, B. S. New Directions in Thermoresponsive Polymers. *Chem. Soc. Rev.* **2013**, *42*, 7214−7243.
(63) Liang, J.; Shan, G.-r.; Pan, P.-j. Aqueous RAFT Polymerization of Acrylamide: A Convenient Method for Polyacrylamide with Narrow Molecular Weight Distribution. *Chin. J. Polym. Sci.* **2017**, *35*, 123−129.
(64) Aerts, A.; Lewis, R. W.; Zhou, Y.; Malic, N.; Moad, G.; Postma, A. Light-Induced RAFT Single Unit Monomer Insertion in Aqueous Solution—Toward Sequence-Controlled Polymers. *Macromol. Rapid Commun.* **2018**, *39*, 1800240.
(65) Terashima, T.; Sugita, T.; Fukae, K.; Sawamoto, M. Synthesis and Single-Chain Folding of Amphiphilic Random Copolymers in Water. *Macromolecules* **2014**, *47* (2), 589−600.

(66) Shibata, M.; Matsumoto, M.; Hirai, Y.; Takenaka, M.; Sawamoto, M.; Terashima, T. Intramolecular Folding or Intermolecular Self-Assembly of Amphiphilic Random Copolymers: On-Demand Control by Pendant Design. *Macromolecules* **2018**, *51* (10), 3738−3745.
(67) Imai, S.; Takenaka, M.; Sawamoto, M.; Terashima, T. Self-Sorting of Amphiphilic Copolymers for Self-Assembled Materials in Water: Polymers Can Recognize Themselves. *J. Am. Chem. Soc.* **2019**, *141* (1), 511−519.
(68) Biais, P.; Colombani, O.; Bouteiller, L.; Stoffelbach, F.; Rieger, J. Unravelling the Formation of BAB Block Copolymer Assemblies during PISA in Water. *Polym. Chem.* **2020**, *11*, 4568−4578.
(69) Deane, O. J.; Jennings, J.; Neal, T. J.; Musa, O. M.; Fernyhough, A.; Armes, S. P. Synthesis and Aqueous Solution Properties of Shape-Shifting Stimulus-Responsive Diblock Copolymer Nano-Objects. *Chem. Mater.* **2021**, *33* (19), 7767−7779.
(70) Ratcliffe, L. P. D.; Derry, M. J.; Ianiro, A.; Tuinier, R.; Armes, S. P. A Single Thermoresponsive Diblock Copolymer Can Form Spheres, Worms or Vesicles in Aqueous Solution. *Angew. Chemie - Int. Ed.* **2019**, *58*, 18964−18970.
(71) Chanamai, R.; Horn, G.; McClements, D. J. Influence of Oil Polarity on Droplet Growth in Oil-in-Water Emulsions Stabilized by a Weakly Adsorbing Biopolymer or a Nonionic Surfactant. *J. Colloid Interface Sci.* **2002**, *247* (1), 167−176.
(72) Liu, D.; Li, C.; Zhang, X.; Yang, F.; Sun, G.; Yao, B.; Zhang, H. Polarity Effects of Asphaltene Subfractions on the Stability and Interfacial Properties of Water-in-Model Oil Emulsions. *Fuel* **2020**, *269*, 117450.

NOTE ADDED AFTER ASAP PUBLICATION

This paper posted online October 28, 2022, with an error in the title. The corrected version was reposted October 28, 2022.

https://doi.org/10.1021/acssuschemeng.2c04354
ACS Sustainable Chem. Eng. 2022, 10, 14806−14816